PHYSICAL REVIEW E **82**, 046701 (2010)

Higher-order Galilean-invariant lattice Boltzmann model for microflows: Single-component gas

Wahyu Perdana Yudistiawan,[1] Sang Kyu Kwak,[1] D. V. Patil,[2] and Santosh Ansumali[1,2]
[1]*Division of Chemical and Biomolecular Engineering, School of Chemical and Biomedical Engineering, Nanyang Technological University, 637459 Singapore, Singapore*
[2]*Engineering Mechanics Unit, Jawaharlal Nehru Centre for Advanced Scientific Research, Jakkur, Bangalore 560064, India*
(Received 20 May 2009; revised manuscript received 25 August 2010; published 5 October 2010)

We introduce a scheme which gives rise to additional degree of freedom for the same number of discrete velocities in the context of the lattice Boltzmann model. We show that an off-lattice D3Q27 model exists with correct equilibrium to recover Galilean-invariant form of Navier-Stokes equation (without any cubic error). In the first part of this work, we show that the present model can capture two important features of the microflow in a single component gas: Knudsen boundary layer and Knudsen Paradox. Finally, we present numerical results corresponding to Couette flow for two representative Knudsen numbers. We show that the off-lattice D3Q27 model exhibits better accuracy as compared to more widely used on-lattice D3Q19 or D3Q27 model. Finally, our construction of discrete velocity model shows that there is no contradiction between entropic construction and quadrature-based procedure for the construction of the lattice Boltzmann model.

DOI: 10.1103/PhysRevE.82.046701 PACS number(s): 47.11.−j, 05.20.Dd

I. INTRODUCTION

The lattice Boltzmann (hereafter LB) method has emerged as an alternate viable tool to model a range of hydrodynamic applications [1–8]. By now, it is understood that the LB model constitutes a well-defined hierarchy of approximation to the Boltzmann equation based on discrete velocity sets and is naturally equipped with relevant boundary conditions derived from Maxwell-Boltzmann theory [9–11]. A lot of attention was given recently to the use of LB models for simulation of gaseous flows in microdevices, where hydrodynamic approximation breaks down [9,12–18]. Although, so far lower-order LB model is massively used in practice, recent works have indicated that the higher-order LB models perform much better for resolving complex phenomena such as Knudsen boundary layer [18], gaseous flow in small devices [19], thermal flows [20], and even in the case of turbulence [21]. In the case of turbulence better performance seems to be originating from the fact that the hydrodynamic limit of the higher-order LB models is Galilean invariant [21]. In order to recover the Galilean-invariant hydrodynamics, it is crucial to have correct equilibrium third order moment at least up to the third order in the Mach number [21–23] (the term *correct* here means same as that obtained from Maxwell-Boltzmann distribution). The Galilean invariance of a general class of LB models has been demonstrated using numerical experiments in Refs. [24,25].

The basic idea that the LB method is an approximate, but a systematic technique for solving the Boltzmann BGK equation with increasing accuracy was proposed in Ref. [26]. Later, in Ref. [10], it was shown that the LB method approximates the Boltzmann BGK equation in terms of the Hermite polynomials similar to the Grad's moment method [27]. This idea was refined further in Refs. [11,15], which showed that it is possible to formulate the LB method in a thermodynamically consistent fashion [8,28–32], in a way similar to the entropic formulation of the Grad's moment method [33]. In these approaches, higher-order discrete velocity models are constructed from roots of Hermite polynomials [11]. However, the roots of the Hermite polynomials are irrational, and the corresponding discrete velocities cannot be fitted into a regular space-filling lattice. Recently, this problem was resolved by pointing out that a rational number approximations of the Hermite quadrature is possible for constructing computationally convenient on-lattice models [22,23]. A few other examples of higher-order on-lattice LB models were also given in Refs. [34,35].

This route of working with the rational number approximation of the Hermite polynomial is quite convenient for the turbulence modeling [21–23]. However, it might just add extra computational cost with less appreciable gain in mixture and/or microflow modeling. In the case of the mixture modeling, this happens because even for the lower-order LB model (D2Q9 model) it is not always possible to match the spatial discretization with the discrete velocity set for all the components (see for example [36]). Similarly, for the microflow modeling the accuracy of the discretization in the velocity space is more crucial (see for example [37]). Thus unlike turbulence, for microflows better accuracy and efficient implementation for the space derivative is a secondary issue. For example it is well known that the Knudsen layer can be observed with the minimum of 16 discrete velocities (which in 3D implies 64 velocities) when the LB method is constructed via the route of Gauss-Hermite quadrature [18,37]. It is interesting to note here that even this particular higher-order LB model fails to reproduce Knudsen paradox phenomena [37]. In fact, numerical studies suggest that a very high order LB model is needed to reproduce the Knudsen minima correctly [37]. Thus, in order to model microflows, it will be quite useful to have a higher-order LB model with a reduced velocity set (as compared to the Gauss-Hermite quadrature route).

In the one-dimensional case, the issue of minimal discrete velocity is well settled. It is understood that Galilean-invariant hydrodynamics for the one-dimensional LB model is possible with the minimum of 4 velocities, provided they are chosen using the Gauss-Hermite quadrature route [15,22]. Recently, it was shown that a rational number approximation with 5 discrete velocities allows an on-lattice

model with the same accuracy [22]. This agrees with the usual understanding that the Gauss-Hermite quadrature is optimal in one-dimension [10,15]. A remarkable result was obtained in Refs. [21,23], where it was shown that in three dimension it is possible to construct an on-lattice model with the Galilean-invariant hydrodynamics with a velocity set of just 41 members. On the other hand, the tensor-product based Gauss-Hermite quadrature route requires a velocity set of 64 members [15]. A more compact 39-speed LB model was given in [35]. Here, we remind that in multidimensional case, discrete velocity vectors are obtained by taking tensor products of the one-dimensional velocity set. This result demonstrated that in the multidimensional case tensor-product based Gauss-Hermite quadrature is suboptimal. Indeed, a similar result is known for lower-order LB models too. In the case of lower-order models (accurate up to the third order in Mach number), while the tensor-product based Gauss-Hermite route requires 27 discrete velocities in three dimension [15], two subsets of set with either 15 or 19 discrete velocities are sufficient to construct models with the same accuracy in the hydrodynamic limit. This important observation that the tensor-product based Gauss-Hermite quadrature route is suboptimal for the construction of the LB models, is the starting point for the current work.

Indeed suboptimality of the tensor-product based Hermite Polynomial in multidimensional case is discussed in detail by [38]. In Ref. [38], it was shown that quadratures with predefined nodes can be constructed by solving appropriate orthogonality conditions. In the context of lattice Boltzmann such a possibility that existing higher-order LBM are not optimal is discussed by [35] and recently explored in great details for all possible on–lattice cases by [21,23,39]. In fact, in Ref. [38], a detailed list of two- and three-dimensional grids which are compact compared to Hermite representation is reported. Theoretical possibilities of using these compact grids for LB were discussed in Ref. [35]. However, such compact grids were never used in the lattice Boltzmann context mostly because they are off-lattice and stability on such off-lattice alternate is not well tested. Thus, recently all possible alternate which are on lattice is explored in Refs. [21,23,39]. Furthermore, such choices of lattices in LBM is on trial and error basis, where grids are chosen from consideration of Gaussian quadrature and is thrown away if it is not stable enough. For higher-order on-lattice models, it is shown in great details that a lattice considered from quadrature prospective is trustworthy only if appropriate H-function (relevant for hydrodynamics) exist on that lattice [21–23]. In Ref. [35] using quadrature route, remarkable result was found that in contrast to result of Ref. [23] (which uses pruning of an entropy equipped lattice), it is possible to construct an on-lattice model with sixth order accuracy by using just 39-discrete velocity set. Although, the link between 39 velocity model and entropic models remains an open question.

To summarize, so far, in the lattice Boltzmann literature three different approaches to construct higher-order lattices were used. These approaches are tensor-product based Gauss-Hermite quadrature route, projection of Gauss-Hermite quadrature on a predefined lattice with appropriate orthogonality condition (as defined in Ref. [38]), and pruning of an entropy equipped tensor-product lattice. Recent works [21–23,35,39] have shown that the first approach of constructing multidimensional Gauss-Hermite quadrature via tensor product is clearly suboptimal. It seems that second approach of projected Gauss-Hermite quadrature on appropriate lattice and third approach of pruning of an entropy equipped tensor-product lattice are two unrelated independent route. The reason being in principle it might be possible to find a lattice which is consistent with quadrature but not consistent with the entropy principle. As stated in Ref. [39]: "Although a number of high-order lattices are obtained using the different approaches and found to be very effective in extending the application domain of the LB method, the comprehensiveness and minimality of those lattices have not been established in general, neither are the connections among the different approaches identified."

In this work we show that as conjectured in Ref. [39], there is no contradiction between the entropic lattice Boltzmann route and the quadrature route. In order to do so, in the present work, an alternate framework to create discrete velocity set is suggested. In this framework, unlike Ref. [35,38,39], the construction of quadrature is given a thermodynamic interpretation. Furthermore, in contrast to Refs. [21–23] a new way of grid construction, which does not rely on pruning of tensor-product based grid, in framework of the entropic lattice Boltzmann is proposed. It is shown that in this framework the entropic formulation of the LB method can be naturally extended to obtain a discrete velocity set with a given accuracy. As an example, a 27-velocity LB model with the Galilean-invariant hydrodynamic limit is derived. The result shows that the new 27-velocity LB model uses same grid as proposed in Ref. [38]. In that respect, our results can also be interpreted as thermodynamic justification of higher-order quadrature as proposed by [38].

Furthermore, in the present work we have extended the set of known analytical solution for the microflow as started in Ref. [18]. Our theoretical and numerical work clearly indicate that off-lattice $D3Q27$ model is far more superior to $D3Q27$ model used in the lattice Boltzmann setting.

The present work is organized as follows: in Sec. II a brief review of the LB method is presented. In Sec. III, a new construction framework for deriving the entropic LB models with arbitrary accuracy and the relevant H-function is presented. In Sec. IV, a 27-velocity LB model with the sixth order accuracy is derived using the new framework. In Secs. V and VI, an appropriate isothermal and thermal equilibrium distribution for the discrete velocity model is derived respectively. In Sec. VII, the moment representation of the kinetic equation is presented. In Sec. VIII, the hydrodynamic limit of the discrete velocity model is derived to show that the Galilean-invariant hydrodynamics is recovered. In Sec. IX, the formal solution for the case of the unidirectional stationary flow is presented and the diffusive boundary condition is used to obtain an explicit solution for the pressure driven and the Couette flow. These results are analyzed further in the Secs. X and XI. An illustrative numerical example has been presented in Sec. XII. Finally, in Sec. XIII a brief discussion on the conclusions and outlook of the present work is provided.

II. LATTICE BOLTZMANN METHOD

Discrete velocity models are often used in the kinetic theory of gases to describe the propagation of shock waves [40]. Motivated by the search for the computationally effective microscopic schemes for the hydrodynamics, the concept of discrete kinetic modeling was revived in Ref. [41]. In this pioneer work, it was shown that indeed a simple discrete kinetic model on lattice can describe the Navier-Stokes hydrodynamics in appropriate limits. The key new idea was to provide a reduced description of the molecular motion, sufficient to describe the hydrodynamics at desired length scales, by considering pseudoparticle dynamics, where particles are constrained to move along some fixed discrete direction only. This concept was refined further in Refs. [1–3] to obtain the LB model, a viable hydrodynamic simulation tool for the Navier-Stokes equations. In its typical formulation, one works with a set of discrete populations $f=\{f_i\}$ corresponding to the predefined discrete velocities $\mathbf{c}_i(i=1,\cdots,N)$ to represent the system. For this set of discrete populations, the evolution equation is often written in the BGK-form [42] as

$$f_i(\mathbf{x}+\mathbf{c}\Delta t,t+\Delta t)=f_i(\mathbf{x},t)+2\beta\{f_i^{\mathrm{eq}}[f(\mathbf{x},t)]-f_i(\mathbf{x},t)\}, \quad (1)$$

where, β denotes the discrete relaxation time and f_i^{eq}, a functional of f, is chosen in such a way that the correct hydrodynamic limit is recovered.

In the last few years, a lot of attention was paid on the construction of the appropriate equilibrium distribution in the discrete case. It was shown that it is possible to construct discrete analog of the Maxwell-Boltzmann distribution by proper choice of the H-function (a necessity to ensure thermodynamic consistency) [11,15,28–32]. As this extension, broadly known as the entropic LB method, is a generalization of the usual LB method, we will not distinguish between the two formulations in the present discussion but present the result for entropic formulations only.

Another crucial ingredient in LB modeling is the choice of the set of discrete velocities itself. An important progress was made in Refs. [10,43,44], where it was shown that the LB method is an approximate technique for solving the Boltzmann BGK equation,

$$\partial_t f_i + c_{i\alpha}\partial_\alpha f_i = -\frac{1}{\tau}[f_i - f_i^{eq}(f)], \quad (2)$$

in the low Mach number limit. Here, τ is the relaxation time, the set of discrete velocities are typically chosen as the root of Hermite polynomials, and a low Mach number expansion of the Maxwell-Boltzmann distribution evaluated at the node of quadrature is used as discrete equilibrium f_i^{eq}. However, the problem with this approach was that one cannot ensure positivity of the f_i^{eq}. In order to fix this deficiency, the framework was later generalized to get the entropic LB method [11,15], where it was shown that it is sufficient to discretize the continuous H-function using the Gauss-Hermite quadrature as

$$H=\sum_{i=1}^{N} f_i\left[\ln\left(\frac{f_i}{w_i}\right)-1\right], \quad w_i>0, \quad (3)$$

with w_i as weights associated with quadrature and f_i^{eq} as minimum of this H-function under the constraint of the local conservation. For example, in the case of isothermal hydrodynamics, we have the conservation law for the mass density, ρ, and the momentum density, J_α, defined as

$$\rho=\sum_{i=1}^{N} f_i, \quad J_\alpha=\sum_{i=1}^{N} f_i c_{i\alpha}. \quad (4)$$

So, in this case the equilibrium can be obtained as minimizer of the H-function [Eq. (3)] under the constraint of the fixed mass and the momentum density [Eq. (4)]. An explicit solution of this minimization problem for the commonly used lattices of the LB method is presented in Ref. [11]. This approach was generalized further in Ref. [22], where it was shown that the rational number approximation of the model allows an on-lattice model with the same accuracy albeit with increased number of discrete velocities. Later, in Refs. [21,23], it was shown that in the multi-dimensional case number of discrete velocities can be drastically reduced by considering only a subset of the set of discrete velocities generated via the tensor product of the desired one-dimensional set. These results suggest that the route of three-dimensional lattices as a tensor product of one-dimensional lattices is far from being optimal. Although it is possible to construct a reduced set by pruning of tensor-product lattice [21,23], it is not obvious that this route is optimal. In the subsequent sections, we will demonstrate that it is possible to create a desired velocity set entirely from multi-dimensional considerations and such a route leads to a discrete velocity set with much reduced number of discrete velocities.

III. ENTROPIC QUADRATURE METHOD

In this section, we propose a set of ansatz needed to construct a discrete velocity set equipped with H-function directly in multidimensional case. These ansatz should be understood as culmination of the set of the rules developed to derive the entropic LB method [11,15,21–23,28–32,45,46]. Before discussing these ansatz, it is important to define a few higher-order moments. In particular, typical to the Grad type moment system [27], We define relevant second, third, and fourth order moments, respectively, as follows:

$$P_{\alpha\beta}=\sum_{i=1}^{N} f_i\left(c_{i\alpha}c_{i\beta}-\frac{k_B T_0}{m}\delta_{\alpha\beta}\right),$$

$$Q_{\alpha\beta\gamma}=\sum_{i=1}^{N} f_i\left\{c_{i\alpha}c_{i\beta}c_{i\gamma}-\frac{k_B T_0}{m}(\delta_{\alpha\beta}c_{i\gamma}+\delta_{\alpha\gamma}c_{i\beta}+\delta_{\beta\gamma}c_{i\alpha})\right\},$$

$$R_{\alpha\beta\gamma\theta} = \sum_{i=1}^{N} f_i \Bigg\{ c_{i\alpha}c_{i\beta}c_{i\gamma}c_{i\theta} + \left(\frac{k_B T_0}{m}\right)^2 (\delta_{\alpha\beta}\delta_{\gamma\theta} + \delta_{\theta\alpha}\delta_{\gamma\beta} + \delta_{\theta\beta}\delta_{\gamma\alpha}) - \frac{k_B T_0}{m}(c_{i\alpha}c_{i\beta}\delta_{\gamma\theta} + c_{i\alpha}c_{i\theta}\delta_{\gamma\beta} + c_{i\alpha}c_{i\gamma}\delta_{\beta\theta} + c_{i\beta}c_{i\theta}\delta_{\gamma\alpha} + c_{i\beta}c_{i\gamma}\delta_{\theta\alpha} + c_{i\gamma}c_{i\theta}\delta_{\beta\alpha}) \Bigg\}, \tag{5}$$

where, T_0 is some reference temperature, k_B is the Boltzmann constant and m is the mass of the particle. It is often convenient to work with reduced fourth order moment defined as,

$$R_{\alpha\beta} = \sum_{i=1}^{N} f_i \Bigg\{ c_i^2 \left(c_{i\alpha}c_{i\beta} - \frac{k_B T_0}{m}\delta_{\alpha\beta} \right) + 5\left(\frac{k_B T_0}{m}\right)^2 \delta_{\alpha\beta} - \frac{7k_B T_0}{m} c_{i\alpha}c_{i\beta} \Bigg\}. \tag{6}$$

Here, we present the necessary set of ansatz as:

(1) *Condition on Equilibrium Moments.* Ideally, we would like that the equilibrium values of the second order moment $P_{\alpha\beta}$, third order moment $Q_{\alpha\beta\gamma}$ and contracted fourth order moment $R_{\alpha\beta}$ are the same as those obtained from the Maxwell-Boltzmann distribution, i.e.,

$$P^{\mathrm{MB}}_{\alpha\beta} = \frac{1}{\rho} J_\alpha J_\beta, \quad Q^{\mathrm{MB}}_{\alpha\beta\gamma} = \frac{1}{\rho^2} J_\alpha J_\beta J_\gamma, \quad R^{\mathrm{MB}}_{\alpha\beta} = \frac{1}{\rho^2} J_\alpha J_\beta J^2. \tag{7}$$

However, typically in a discrete velocity model, the equilibrium distributions will satisfy such conditions in an asymptotic sense only. So, we would like that these conditions are satisfied at least up to the fourth order in Mach number, i.e., $\mathcal{O}(u^4)$. This is sufficient to recover the Galilean-invariant hydrodynamics [23].

(2) *Discrete H-function.* It is sufficient to consider the discrete H-function of the Kullback form as given by, Eq. (3). Here, the weights w_i are unknown positive definite numbers. The formal expression for the equilibrium distribution (in isothermal setting, where energy conservation is not considered) is

$$f_i^{eq} = w_i \exp(\alpha + \beta_\theta c_{i\theta}) \equiv w_i A \rho \exp(\beta_\theta c_{i\theta}), \tag{8}$$

where, α and β_θ are the Lagrange multipliers associated with the mass and momentum conservation and $A = \rho^{-1} \exp \alpha$ with $A > 0$. We need to determine these weights such that the equilibrium distribution has desired higher-order moments (See Eq. (7)). Indeed these two ansatz were used earlier in Refs. [22,23] to construct on-lattice higher-order discrete Boltzmann equation.

(3) *Constraints on weights.* We claim that in order to satisfy first two ansatz [Eqs. (7) and (3)], it is sufficient that apart from positivity constraint ($w_i > 0$), weights also obey following set of constraints on the even moments,

$$\sum_{i=1}^{N} w_i = 1, \quad \sum_{i=1}^{N} w_i c_{i\alpha}c_{i\beta} = \left(\frac{k_B T_0}{m}\right)\delta_{\alpha\beta},$$

$$\sum_{i=1}^{N} w_i c_{i\alpha}c_{i\beta}c_{i\gamma}c_{i\zeta} = \left(\frac{k_B T_0}{m}\right)^2 \Delta_{\alpha\beta\gamma\zeta},$$

$$\sum_{i=1}^{N} w_i c_{i\alpha}c_{i\beta}c_{i\gamma}c_{i\zeta}c_{i\eta}c_{i\theta} = \left(\frac{k_B T_0}{m}\right)^3 \Delta_{\alpha\beta\gamma\zeta\eta\theta}, \tag{9}$$

where, symbol Δ is used to denote symmetrized tensor generated from the Kronecker-delta. In particular,

$$\Delta_{\alpha\beta\gamma\zeta} = \delta_{\alpha\beta}\delta_{\gamma\zeta} + \delta_{\alpha\gamma}\delta_{\beta\zeta} + \delta_{\alpha\zeta}\delta_{\beta\gamma},$$

$$\Delta_{\alpha\beta\gamma\zeta\eta\theta} = \delta_{\alpha\beta}\Delta_{\gamma\zeta\eta\theta} + \delta_{\alpha\gamma}\Delta_{\beta\zeta\eta\theta} + \delta_{\alpha\zeta}\Delta_{\beta\gamma\eta\theta} + \delta_{\alpha\eta}\Delta_{\beta\gamma\zeta\theta} + \delta_{\alpha\theta}\Delta_{\beta\gamma\zeta\eta}. \tag{10}$$

The set of conditions on the odd moments are

$$\sum_{i=1}^{N} w_i c_{i\alpha} = 0, \quad \sum_{i=1}^{N} w_i c_{i\alpha}c_{i\beta}c_{i\gamma} = 0,$$

$$\sum_{i=1}^{N} w_i c_{i\alpha}c_{i\beta}c_{i\gamma}c_{i\zeta}c_{i\eta} = 0,$$

$$\sum_{i=1}^{N} w_i c_{i\alpha}c_{i\beta}c_{i\gamma}c_{i\zeta}c_{i\eta}c_{i\theta}c_{i\kappa} = 0. \tag{11}$$

As stated earlier, the condition on the equilibrium moments are satisfied up to the accuracy of $\mathcal{O}(u^4)$ only. In fact, it can be easily proven that this ansatz is just a direct consequence of the previous two ansatz. The equivalence of the first two constraints with the third one is one of the central results of the present work. The practical consequence of this ansatz is that the problem of finding reliable entropic LB model is simplified to solving a set of algebraic equations coupled with positivity constraints. We defer the proof of this equivalence to later sections and propose few more ansatz, which will allow an analytically solvable set of algebraic equations.

(4) *Energy Dependent Weights.* Any meaningful set of discrete velocities is composed by choosing discrete velocities with different energy $E \equiv c_x^2 + c_y^2 + c_z^2$. Thus, a convenient notation of energy shell was introduced in the Ref. [30]. We assume that the weights, w_i, are just a function of energy, E. In fact, all existing LB models satisfy this criteria.

(5) *Symmetry Group of the Lattice.* For any discrete velocity set $\mathcal{C}$, we must have following,

(i) *Closure under Inversion.* if a discrete velocity $\mathbf{c}_i \equiv (c_{ix}, c_{iy}, c_{iz})$ is an element of the set i.e., $\mathbf{c}_i \in \mathcal{C}$, then $-\mathbf{c}_i \in \mathcal{C}$. This closure, coupled with the ansatz 4, trivially ensures that Eq. (11) is satisfied.

(ii) *Closure under Reflection.* If a discrete velocity $\mathbf{c}_i \equiv (c_{ix}, c_{iy}, c_{iz})$ is an element of the set i.e., $\mathbf{c}_i \in \mathcal{C}$, then all possible reflection of it are also a member of the set [i.e., $(\pm c_{ix}, \pm c_{iy}, \pm c_{iz}) \in \mathcal{C}$]. The first condition is just a special case of the second one. Thus, any discrete velocity set con-

structed in this way will satisfy Eq. (11) trivially. Furthermore, as this condition ensures that there is no preference on a specific direction, so for any natural number n and m,

$$\sum_{i=1}^{N} c_{ix}^{2n} = \sum_{i=1}^{N} c_{iy}^{2n} = \sum_{i=1}^{N} c_{iz}^{2n},$$

$$\sum_{i=1}^{N} c_{ix}^{2n} c_{iy}^{2m} = \sum_{i=1}^{N} c_{ix}^{2n} c_{iz}^{2m} = \sum_{i=1}^{N} c_{iy}^{2n} c_{iz}^{2m}. \tag{12}$$

This means in order to satisfy conditions on even moments [Eq. (9)], it is sufficient to satisfy 7 scalar equations,

$$\sum_{i=1}^{N} w_i = 1, \quad \sum_{i=1}^{N} w_i c_{ix}^2 = \frac{k_B T_0}{m},$$

$$\sum_{i=1}^{N} w_i c_{ix}^4 = 3\left(\frac{k_B T_0}{m}\right)^2,$$

$$\sum_{i=1}^{N} w_i c_{ix}^2 c_{iy}^2 = \left(\frac{k_B T_0}{m}\right)^2,$$

$$\sum_{i=1}^{N} w_i c_{ix}^6 = 15\left(\frac{k_B T_0}{m}\right)^3,$$

$$\sum_{i=1}^{N} w_i c_{ix}^2 c_{iy}^4 = 3\left(\frac{k_B T_0}{m}\right)^3,$$

$$\sum_{i=1}^{N} w_i c_{ix}^2 c_{iy}^2 c_{iz}^2 = \left(\frac{k_B T_0}{m}\right)^3. \tag{13}$$

We therefore need at least seven degree of freedom in the model to obtain the sixth order accuracy.

IV. CONSTRUCTION OF VELOCITY SET

The ansatz 5 mentioned in the previous section is trivially satisfied if we sample the discrete velocities from the cubic bravice lattice. Thus, apart from the zero energy vector ($\mathbf{c}=\{0,0,0\}$) other simple choices to generate energy shell is to sample discrete velocities from either of the three cubic lattices, i.e., simple cubic (SC), face-centered cubic (FCC), or body-centered cubic (BCC) structures [47]. Here, we remind the reader that we need to satisfy seven nonlinear algebraic equations along with inequalities $w_i > 0$. As any energy shell has two degrees of freedom (magnitude of the energy and weight associated with the shell), apart from zero energy shell, we need to have at least three more energy shells.

The energy shells are chosen via a trial-and-error procedure. Only available guideline is that one would like to have as few as possible energy shells and within the energy shell the number of the discrete velocities being as few as possible. The optimal choice is to choose three energy shells from the SC structure. However, that set is inadmissible as

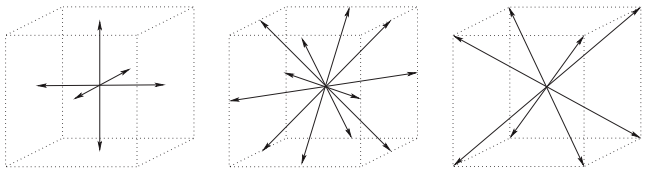

FIG. 1. Admissible energy shells: notice that unlike typical $D3Q27$ lattice Boltzmann model we are not assuming that magnitude of energy are in ratio 1:2:3.

weights are negative for that choice. However, it is possible to satisfy all equations with positive values of the weights if we chose each of the three energy shells from different structure simultaneously (one each from SC, FCC, and BCC structure, see Fig. 1). Thus, instead of assuming that the magnitude of energy are in ratio of 1:2:3, we put it as $a^2:2b^2:3d^2$, where a, b, and d are the distortion parameters. Denoting w_0, w_a, w_b, and w_d being weights corresponding to shell with energy zero, a^2, $2b^2$, and $3d^2$, respectively, Eq. (13) may be simplified. Further, the last two conditions on sixth moments (Eq. (13)) may be solved to obtain,

$$w_d = \frac{1}{8d^6}\left(\frac{k_B T_0}{m}\right)^3, \quad w_b = \frac{1}{2b^6}\left(\frac{k_B T_0}{m}\right)^3, \tag{14}$$

which when substituted in a condition for fourth moment [Eq. (13)] gives

$$w_a = \frac{1}{a^4}\left[1 - \frac{1}{b^2}\left(\frac{k_B T_0}{m}\right)\right]\left(\frac{k_B T_0}{m}\right)^2, \quad \frac{2}{b^2} + \frac{1}{d^2} = \left(\frac{k_B T_0}{m}\right)^{-1}. \tag{15}$$

Furthermore, when substituted in second moment equation gives,

$$d^2 + b^2 = 2a^2. \tag{16}$$

Finally, the first condition on sixth order moment gives,

$$a^6 w_a = 5\left(\frac{k_B T_0}{m}\right)^3. \tag{17}$$

It is this condition, which differentiate the current model from standard $D3Q27$ model. If, we do not insist on this condition, we may impose the condition $a=b=c$ to obtain,

$$a = b = c = \sqrt{\frac{3k_B T_0}{m}}, \tag{18}$$

which gives the standard $D3Q27$ model. Further, we note that from Eqs. (15) and (16), a^2 and d^2 may be written in terms of b^2 as

$$a^2 = \frac{b^2}{2}\frac{b^2 - \frac{k_B T_0}{m}}{b^2 - 2\frac{k_B T_0}{m}}, \quad d^2 = \frac{b^2 \frac{k_B T_0}{m}}{b^2 - 2\frac{k_B T_0}{m}}. \tag{19}$$

Insisting on Eq. (17) gives a system of equations. So, finally we obtain two valid solutions, referred as Basis 1 and Basis 2, (which satisfy $w_i > 0$) corresponding to

$$b = \sqrt{6 \pm \sqrt{15}}. \tag{20}$$

In this way, we can see that given the constraints, we are left with only one parameter to tune, which is b. Conditional upon $b^2 > 2\frac{k_B T_0}{m}$, we may see that a^2 and d^2 are always positive and thus always have solution(s). At $b^2 = 3\frac{k_B T_0}{m}$ we recover the normal $D3Q27$ model, with $a^6 w_a = 4(\frac{k_B T_0}{m})^3$ as opposed to $5(\frac{k_B T_0}{m})^3$ given by Eq. (17). Also note that for $b^2 > 2\frac{k_B T_0}{m}$, we have $a^6 w_a \geq 4(\frac{k_B T_0}{m})^3$. Hence, at this juncture, it is pertinent to compare the current choice of 27-velocity LB model with the usual Hermite based $D3Q27$ model (see for example [11]). In the usual $D3Q27$ model, the three energy shell are sampled from the same cube, so energy of the shells are in the ratio 1:2:3. As fixation of the energy ratio will reduce the available degrees of freedom, it is clear that usual $D3Q27$ model fails to satisfy all the seven conditions. However, in the current case no such restriction is imposed, so we have managed to satisfy all seven conditions on the moment of the weights [Eq. (13)]. However, the penalty is that the discrete velocity set is no longer space-filling. Thus, compared to usual $D3Q27$ model, the implementation of the advection will be nontrivial.

V. ISOTHERMAL EQUILIBRIUM DISTRIBUTION

In this section, the explicit expression for the equilibrium distribution [Eq. (8)] is presented. Our task here is to find the Lagrange multipliers using Eq. (4) in terms of conserved moments ρ and u_θ. For this nonlinear problem, the explicit solution is not available. However, we know that at zero velocity ($u_\theta = 0$), the Lagrange multipliers are $A = 1$, $\beta_\theta = 0$.

Since, LB method works in subsonic region where Mach number is considerably small, we can take the Mach number (velocity) to be the smallness parameter, and work out a perturbative scheme around the zero velocity. So we introduce a formal smallness-parameter, ϵ, which may also be termed as a book-keeping parameter (this is because, at the end of the perturbation analysis is set equal to 1) and write,

$$A = 1 + \epsilon A^{(1)} + \epsilon^2 A^{(2)} + \epsilon^3 A^{(3)} + \epsilon^4 A^{(4)} + \epsilon^5 A^{(5)} + \epsilon^6 A^{(6)} + \cdots,$$

$$\beta_\theta = \epsilon B_\theta^{(1)} + \epsilon^2 B_\theta^{(2)} + \epsilon^3 B_\theta^{(3)} + \epsilon^4 B_\theta^{(4)} + \epsilon^5 B_\theta^{(5)} + \epsilon^6 B_\theta^{(6)} + \cdots. \tag{21}$$

Upon substituting above expansion in Eq. (8) and coupled with Eq. (4), we obtain a solution up to sixth order of ϵ (at $\epsilon = 1$),

$$A = 1 - \frac{u^2}{\left(\frac{k_B T_0}{m}\right)} + \frac{u^4}{\left(\frac{k_B T_0}{m}\right)^2} - \frac{u^6}{\left(\frac{k_B T_0}{m}\right)^3} + \mathcal{O}(u^8),$$

$$\beta_\theta = \frac{u_\theta}{\left(\frac{k_B T_0}{m}\right)} + \mathcal{O}(u^7). \tag{22}$$

Finally the higher-order moment can be computed to obtain,

$$P_{\alpha\beta}^{\mathrm{eq}} - P_{\alpha\beta}^{\mathrm{MB}} = \mathcal{O}(u^6),$$

$$Q_{\alpha\beta\gamma}^{\mathrm{eq}} - Q_{\alpha\beta\gamma}^{\mathrm{MB}} = \mathcal{O}(u^5),$$

$$R_{\alpha\beta}^{\mathrm{eq}} - R_{\alpha\beta}^{\mathrm{MB}} = \mathcal{O}(u^4). \tag{23}$$

Hence, the desired moments up to order $\mathcal{O}(u^4)$ are recovered. This shows, it is sufficient that the discrete velocity models satisfy the ansatz 2 and 3.

VI. THERMAL EQUILIBRIUM DISTRIBUTION

In this section, we try to construct an energy conserving model because the off-lattice is higher-order accurate model. This requires the inclusion of energy conservation along with the mass and momentum conservation constraint. This means the function to be minimized is

$$\Theta = \int \left\{ f_i \left[\ln\left(\frac{f_i}{w_i}\right) - 1 \right] - \alpha f_i - \beta_\theta c_{i\theta} f_i - \gamma c_i^2 f_i \right\} dc_i, \tag{24}$$

where, α, β_θ, and γ are the Lagrange multipliers associated with the mass, momentum and energy conservation, respectively. Here, we present an explicit expression for the thermal equilibrium distribution. For an algebraic convenience we rewrite the formal expression of the equilibrium distribution as

$$f_i^{\mathrm{eq}} = w_i \rho \exp(\alpha + \beta_\theta c_{i\theta} + \gamma c_i^2). \tag{25}$$

The way we have constructed the model ensures that at zero velocity and $T = T_0$, we have

$$f_i^{\mathrm{eq}}(\mathbf{u} = 0, T = T_0) = w_i \rho. \tag{26}$$

Hence, we have to solve following the system of equations:

$$\sum_i f_i^{\mathrm{eq}} = \rho,$$

$$\sum_i f_i^{\mathrm{eq}} c_{i\beta} = \epsilon \rho u_\beta,$$

$$\sum_i f_i^{\mathrm{eq}} c_i^2 = \epsilon^2 \rho u^2 + 3p_0 + 3\eta(p - p_0). \tag{27}$$

Further, using the perturbative procedure as per in Sec. V, we get an expression for thermal equilibrium as

$$\begin{aligned} f_i^{\mathrm{eq}} = w_i \rho \Bigg\{ & 1 + \frac{u_\alpha c_{i\alpha}}{T_0}\left[1 - \left(\frac{T}{T_0} - 1\right)\right] + \frac{1}{2}\left(\frac{1}{T_0} c_i^2 - 3\right)\left(\frac{T}{T_0} - 1\right) \\ & - \frac{u^2}{2T_0} + \frac{1}{2T_0^2}(u_\alpha c_{i\alpha})^2 - \frac{u_\alpha u^2}{2T_0^2} c_{i\alpha} + \frac{1}{6T_0^3}(u_\alpha c_{i\alpha})^3 \\ & + \frac{u_\alpha c_{i\alpha}}{2T_0}\left(\frac{T}{T_0} - 1\right)\left(\frac{1}{T_0} c_i^2 - 3\right) + \left(\frac{T}{T_0} - 1\right)^2 \left\{ \frac{15}{8} - \frac{5}{4T_0} c_i^2 \right. \\ & \left. + \frac{1}{8T_0^2} c_i^2 c_i^2 \right\} \Bigg\}, \end{aligned} \tag{28}$$

and moments at equilibrium are

$$\sigma_{\alpha\beta}^{\mathrm{eq}} = \rho u_\alpha u_\beta - \frac{1}{3}\rho u^2 \delta_{\alpha\beta},$$

$$q_\alpha^{\mathrm{eq}} = \rho \frac{5}{2} T u_\alpha + \rho u^2 \frac{u_\alpha}{2}. \tag{29}$$

The moments q_α and $\sigma_{\alpha\beta}$ are defined, respectively, as

$$q_\alpha = \frac{1}{2}\sum_{i=1}^{N} f_i c_i^2 c_{i\alpha}, \quad \sigma_{\alpha\beta} = \sum_{i=1}^{N} f_i \overline{c_{i\alpha} c_{i\beta}}, \tag{30}$$

and

$$\overline{c_{i\alpha} c_{i\beta}} = \left[c_{i\alpha} c_{i\beta} - \frac{1}{D} c_i^2 \delta_{\alpha\beta} \right],$$

$$\overline{c_{i\alpha} c_{i\beta} c_{i\gamma}} = \left[c_{i\alpha} c_{i\beta} c_{i\gamma} - \frac{1}{D+2} c_i^2 (\delta_{\alpha\beta} c_{i\gamma} + \delta_{\alpha\gamma} c_{i\beta} + \delta_{\beta\gamma} c_{i\alpha}) \right], \tag{31}$$

where, D being the dimension of space. Also, for sixth order accurate models,

$$\hat{R}^{\mathrm{eq}} = 15\rho T_0^2 \left[1 + 2\left(\frac{T}{T_0} - 1 \right) \right] + 10\rho T_0 u^2,$$

$$\hat{R}_{\alpha\beta} = 7T_0 u_\alpha u_\beta - \frac{7}{3}\rho T_0 u^2 \delta_{\alpha\beta}, \tag{32}$$

where, the moments $\hat{R}$ and $\hat{R}_{\alpha\beta}$ are defined, respectively, as

$$\hat{R} = \sum_{i=1}^{N} f_i c_i^2 c_i^2, \quad \hat{R}_{\alpha\beta} = \sum_{i=1}^{N} f_i c_i^2 \overline{c_{i\alpha} c_{i\beta}}. \tag{33}$$

Thus, we can see that we do recover the desired moments up to the order $\mathcal{O}(u^4)$, which also shows that it is sufficient that discrete velocity models satisfy the ansatz 2 and 3.

VII. MOMENT CHAIN AND RESEMBLANCE TO GRAD'S METHOD

In order to compare the present model with a typical Grad's moment system, it would be convenient to write the moment chain for the present kinetic equation, Eq. (2). As, we have 27 discrete velocities, we can have only 27 independent moments. In this particular setup, we will write it instead in a slightly different form, in such a way that all of moments are still independent after the reduction to the normal $D3Q27$ model (special case where $b = \sqrt{\frac{3k_B T_0}{m}}$). The present model is different than the usual Grad representation, wherein, higher-order moments are included only after the inclusion of all the lower-order moments. The set of 27 independent moments that we choose are

$$M = \{\rho, J_\alpha, P, \sigma_{\alpha\beta}, q_\alpha, \hat{R}, \hat{R}_{\alpha\beta}, \hat{N}_{\alpha\beta\gamma}, \psi\}, \tag{34}$$

where

$$P = \sum_{i=1}^{N} f_i c_i^2, \quad \hat{N}_{\alpha\beta\gamma} = \sum_{i=1}^{N} f_i c_i^2 \overline{c_{i\alpha} c_{i\beta} c_{i\gamma}}, \quad \psi = \sum_{i=1}^{N} f_i c_i^2 c_i^2 c_i^2. \tag{35}$$

As we are dealing with a discrete velocity model system, one can always write the closed form of the moment chain. Once we have decided the choice of independent moments, we can write the moment system. In the present case, they give rise to a closed chain of 27 independent equations, as we have 27 discrete velocities. Here, it needs to be reminded that the energy conservation is absent in an isothermal discrete velocity model. In thermal model, we have balance of mass, momentum and energy as

$$\partial_t \rho + \partial_\alpha J_\alpha = 0,$$

$$\partial_t J_\alpha + \partial_\beta \sigma_{\alpha\beta} + \frac{1}{D}\partial_\alpha P = \rho g_\alpha,$$

$$\partial_t P + 2\partial_\alpha q_\alpha = 0. \tag{36}$$

The evolution equations for the second order moments $\sigma_{\alpha\beta}$ are,

$$\partial_t \sigma_{\alpha\beta} + \partial_\gamma Q_{\alpha\beta\gamma} + \frac{2}{5}(\partial_\alpha q_\beta + \partial_\beta q_\alpha) - \frac{4}{15}\partial_\gamma q_\gamma \delta_{\alpha\beta} = \frac{1}{\tau}(\sigma_{\alpha\beta}^{\mathrm{eq}} - \sigma_{\alpha\beta}). \tag{37}$$

We have equation of motion for the heat-flux, q_α, from the discrete kinetic Eq. (3) as

$$\partial_t q_\alpha + \frac{1}{2}\partial_\beta \left(\hat{R}_{\alpha\beta} + \frac{1}{3}\hat{R}\delta_{\alpha\beta} \right) = \frac{1}{\tau}(q_\alpha^{\mathrm{eq}} - q_\alpha) + \frac{g_\alpha 5 p_0}{2} \tag{38}$$

and we have closure relations for other third order tensorial moments as

$$Q_{xyz} = \frac{1}{3d^2}\hat{N}_{xyz},$$

$$Q_{xyy} - Q_{xzz} = \frac{1}{2b^2}(\hat{N}_{xyy} - \hat{N}_{xzz}),$$

$$Q_{zxx} - Q_{zyy} = \frac{1}{2b^2}(\hat{N}_{zxx} - \hat{N}_{zyy}),$$

$$Q_{xyy} + Q_{xzz} = \frac{1}{3D_1}\left[\left(15b^6 - 78b^4 \left(\frac{k_B T_0}{m} \right) + 63b^2 \left(\frac{k_B T_0}{m} \right)^2 \right) J_x \frac{k_B T_0}{m} - \left(15b^4 - 75b^2 \left(\frac{k_B T_0}{m} \right) + 90 \left(\frac{k_B T_0}{m} \right)^2 \right) \hat{N}_{xxx} - \left(10b^6 - 48b^4 \left(\frac{k_B T_0}{m} \right) \right) \right.$$

$$+ 74b^2\left(\frac{k_BT_0}{m}\right)^2 - 84\left(\frac{k_BT_0}{m}\right)^3\Bigg)q_x\Bigg],$$

$$Q_{yzz} + Q_{yxx} = \frac{1}{3D_1}\Bigg\{\Bigg[15b^6 - 78b^4\left(\frac{k_BT_0}{m}\right) + 63b^2\left(\frac{k_BT_0}{m}\right)^2\Bigg]J_y\frac{k_BT_0}{m} - \Bigg[15b^4 - 75b^2\left(\frac{k_BT_0}{m}\right) + 90\left(\frac{k_BT_0}{m}\right)^2\Bigg]\hat{N}_{yyy} - \Bigg[10b^6 - 48b^4\left(\frac{k_BT_0}{m}\right) + 74b^2\left(\frac{k_BT_0}{m}\right)^2 - 84\left(\frac{k_BT_0}{m}\right)^3\Bigg]q_y\Bigg\}, \tag{39}$$

where

$$D_1 = 4b^6 - 33b^4\left(\frac{k_BT_0}{m}\right) + 116b^2\left(\frac{k_BT_0}{m}\right)^2 - 147\left(\frac{k_BT_0}{m}\right)^3. \tag{40}$$

A. Fourth order moments

The evolution equations for the fourth order moments are

$$\partial_t\hat{R}_{\alpha\beta} - \frac{2}{15}\partial_\gamma n_\gamma\delta_{\beta\alpha} + \partial_\gamma\hat{N}_{\alpha\beta\gamma} + \frac{1}{5}(\partial_\beta n_\alpha + \partial_\alpha n_\beta) = \frac{1}{\tau}(\hat{R}^{\mathrm{eq}}_{\alpha\beta} - \hat{R}_{\alpha\beta}). \tag{41}$$

$$\partial_t\hat{R} + \partial_\gamma n_\gamma = \frac{1}{\tau}(\hat{R}^{\mathrm{eq}} - \hat{R}), \tag{42}$$

where

$$n_\alpha = \sum_{i=1}^{N} f_i c_{i\alpha} c_i^2 c_i^2. \tag{43}$$

B. Fifth order moments

Similarly, following are the evolution equations for the fifth order moments:

$$\partial_t\hat{N}_{xyz} + \frac{2b^2\left(\frac{k_BT_0}{m}\right)}{\left(b^2 - 2\frac{k_BT_0}{m}\right)\left(2b^2 - 7\frac{k_BT_0}{m}\right)}[\partial_x(2b^2\sigma_{yz} - \hat{R}_{yz}) + \partial_y(2b^2\sigma_{xz} - \hat{R}_{xz}) + \partial_z(2b^2\sigma_{xy} - \hat{R}_{xy})] = \frac{1}{\tau}(\hat{N}^{\mathrm{eq}}_{xyz} - \hat{N}_{xyz}) \tag{44}$$

$$\partial_t\hat{N}_{xxx} + \partial_x[r_4P + r_5\hat{R} + r_6\psi + r_7\sigma_{xx} + r_8\hat{R}_{xx}] + \partial_y\Bigg[\frac{-6b^4\left(b^2 - 6\frac{k_BT_0}{m}\right)\frac{k_BT_0}{m}}{5\left(2b^2 - 7\frac{k_BT_0}{m}\right)\left(b^2 - 2\frac{k_BT_0}{m}\right)}\sigma_{xy} + \frac{2b^2\left(b^4 - 4b^2\frac{k_BT_0}{m} - 2\left(\frac{k_BT_0}{m}\right)^2\right)}{5\left(2b^2 - 7\frac{k_BT_0}{m}\right)\left(b^2 - 2\frac{k_BT_0}{m}\right)}\hat{R}_{xy}\Bigg] + \partial_z\Bigg[\frac{-6b^4\left(b^2 - 6\frac{k_BT_0}{m}\right)\frac{k_BT_0}{m}}{5\left(2b^2 - 7\frac{k_BT_0}{m}\right)\left(b^2 - 2\frac{k_BT_0}{m}\right)}\sigma_{xz} + \frac{2b^2\left(b^4 - 4b^2\frac{k_BT_0}{m} - 2\left(\frac{k_BT_0}{m}\right)^2\right)}{5\left(2b^2 - 7\frac{k_BT_0}{m}\right)\left(b^2 - 2\frac{k_BT_0}{m}\right)}\hat{R}_{xz}\Bigg] = \frac{1}{\tau}(\hat{N}^{\mathrm{eq}}_{xxx} - \hat{N}_{xxx}) \tag{45}$$

$$\partial_t\hat{N}_{yyy} + \partial_x\Bigg[\frac{-6b^4\left(b^2 - 6\frac{k_BT_0}{m}\right)\frac{k_BT_0}{m}}{5\left(2b^2 - 7\frac{k_BT_0}{m}\right)\left(b^2 - 2\frac{k_BT_0}{m}\right)}\sigma_{xy} + \frac{2b^2\left(b^4 - 4b^2\frac{k_BT_0}{m} - 2\left(\frac{k_BT_0}{m}\right)^2\right)}{5\left(2b^2 - 7\frac{k_BT_0}{m}\right)\left(b^2 - 2\frac{k_BT_0}{m}\right)}\hat{R}_{xy}\Bigg] + \partial_y[r_4P + r_5\hat{R} + r_6\psi + r_7\sigma_{yy} + r_8\hat{R}_{yy}] + \partial_z\Bigg[\frac{-6b^4\left(b^2 - 6\frac{k_BT_0}{m}\right)\frac{k_BT_0}{m}}{5\left(2b^2 - 7\frac{k_BT_0}{m}\right)\left(b^2 - 2\frac{k_BT_0}{m}\right)}\sigma_{yz} + \frac{2b^2\left(b^4 - 4b^2\frac{k_BT_0}{m} - 2\left(\frac{k_BT_0}{m}\right)^2\right)}{5\left(2b^2 - 7\frac{k_BT_0}{m}\right)\left(b^2 - 2\frac{k_BT_0}{m}\right)}\hat{R}_{yz}\Bigg] = \frac{1}{\tau}(\hat{N}^{\mathrm{eq}}_{yyy} - \hat{N}_{yyy}) \tag{46}$$

$$
\begin{aligned}
&\partial_t \hat{N}_{zzz} + \partial_x \left[\frac{-6b^4\left(b^2 - 6\frac{k_B T_0}{m}\right)\frac{k_B T_0}{m}}{5\left(2b^2 - 7\frac{k_B T_0}{m}\right)\left(b^2 - 2\frac{k_B T_0}{m}\right)} \sigma_{xz} \right. \\
&\quad \left. + \frac{2b^2\left(b^4 - 4b^2\frac{k_B T_0}{m} - 2\left(\frac{k_B T_0}{m}\right)^2\right)}{5\left(2b^2 - 7\frac{k_B T_0}{m}\right)\left(b^2 - 2\frac{k_B T_0}{m}\right)} \hat{R}_{xz} \right] \\
&\quad + \partial_y \left[\frac{-6b^4\left(b^2 - 6\frac{k_B T_0}{m}\right)\frac{k_B T_0}{m}}{5\left(2b^2 - 7\frac{k_B T_0}{m}\right)\left(b^2 - 2\frac{k_B T_0}{m}\right)} \sigma_{yz} \right. \\
&\quad \left. + \frac{2b^2\left(b^4 - 4b^2\frac{k_B T_0}{m} - 2\left(\frac{k_B T_0}{m}\right)^2\right)}{5\left(2b^2 - 7\frac{k_B T_0}{m}\right)\left(b^2 - 2\frac{k_B T_0}{m}\right)} \hat{R}_{yz} \right] \\
&\quad + \partial_z [r_4 P + r_5 \hat{R} + r_6 \psi + r_7 \sigma_{zz} + r_8 \hat{R}_{zz}] \\
&\quad = \frac{1}{\tau}(\hat{N}^{\mathrm{eq}}_{zzz} - \hat{N}_{zzz}) \qquad (47)
\end{aligned}
$$

$$
\begin{aligned}
&\partial_t(\hat{N}_{xzz} - \hat{N}_{xyy}) + \frac{2b^4}{(2b^2 - a^2)}\partial_x[-a^2(\sigma_{zz} - \sigma_{yy}) + \hat{R}_{zz} - \hat{R}_{yy}] \\
&\quad - \frac{2b^4}{(3d^2 - 2b^2)}\partial_y(3d^2\sigma_{xy} - \hat{R}_{xy}) \\
&\quad + \frac{2b^4}{(3d^2 - 2b^2)}\partial_z(3d^2\sigma_{xz} - \hat{R}_{xz}) \\
&\quad = \frac{1}{\tau}(\hat{N}^{\mathrm{eq}}_{xzz} - \hat{N}^{\mathrm{eq}}_{xyy} - \hat{N}_{xzz} + \hat{N}_{xyy}),
\end{aligned}
$$

$$
\begin{aligned}
&\partial_t(\hat{N}_{yxx} - \hat{N}_{yzz}) + \frac{2b^4}{(3d^2 - 2b^2)}\partial_x(3d^2\sigma_{yx} - \hat{R}_{yx}) + \frac{2b^4}{(2b^2 - a^2)} \\
&\quad \times \partial_y[-a^2(\sigma_{xx} - \sigma_{zz}) + \hat{R}_{xx} - \hat{R}_{zz}] \\
&\quad - \frac{2b^4}{(3d^2 - 2b^2)}\partial_z(3d^2\sigma_{yz} - \hat{R}_{yz}) \\
&\quad = \frac{1}{\tau}(\hat{N}^{\mathrm{eq}}_{yxx} - \hat{N}^{\mathrm{eq}}_{yzz} - \hat{N}_{yxx} + \hat{N}_{yzz}),
\end{aligned}
$$

$$
\begin{aligned}
&\partial_t(\hat{N}_{zxx} - \hat{N}_{zyy}) + \frac{2b^4}{(3d^2 - 2b^2)}\partial_x(3d^2\sigma_{xz} - \hat{R}_{xz}) \\
&\quad - \frac{2b^4}{(3d^2 - 2b^2)}\partial_y(3d^2\sigma_{yz} - \hat{R}_{yz}) + \frac{2b^4}{(2b^2 - a^2)} \\
&\quad \times \partial_z[-a^2(\sigma_{xx} - \sigma_{yy}) + \hat{R}_{xx} - \hat{R}_{yy}] \\
&\quad = \frac{1}{\tau}(\hat{N}^{\mathrm{eq}}_{zxx} - \hat{N}^{\mathrm{eq}}_{zyy} - \hat{N}_{zxx} + \hat{N}_{zyy}), \qquad (48)
\end{aligned}
$$

where

$$
r_4 = -\frac{2b^6\left(b^2 - \frac{k_B T_0}{m}\right)\left(b^2 - 3\frac{k_B T_0}{m}\right)}{\left(b^2 - 2\frac{k_B T_0}{m}\right)\left(b^2 - 7\frac{k_B T_0}{m}\right)\left(2b^2 - 7\frac{k_B T_0}{m}\right)\left(3b^2 - 7\frac{k_B T_0}{m}\right)}\left(\frac{k_B T_0}{m}\right),
$$

$$
r_5 = \frac{2b^2\left(b^8 - 6b^6\frac{k_B T_0}{m} + 22b^4\left(\frac{k_B T_0}{m}\right)^2 - 54b^2\left(\frac{k_B T_0}{m}\right)^3 + 49\left(\frac{k_B T_0}{m}\right)^4\right)}{3\left(b^2 - 2\frac{k_B T_0}{m}\right)\left(b^2 - 7\frac{k_B T_0}{m}\right)\left(2b^2 - 7\frac{k_B T_0}{m}\right)\left(3b^2 - 7\frac{k_B T_0}{m}\right)},
$$

$$
r_6 = \frac{2\left(4b^6 - 33b^4\left(\frac{k_B T_0}{m}\right) + 116b^2\left(\frac{k_B T_0}{m}\right)^2 - 147\left(\frac{k_B T_0}{m}\right)^3\right)}{15\left(b^2 - 7\frac{k_B T_0}{m}\right)\left(2b^2 - 7\frac{k_B T_0}{m}\right)\left(3b^2 - 7\frac{k_B T_0}{m}\right)},
$$

$$r_7 = \frac{2b^4\left(b^2 - \frac{k_BT_0}{m}\right)\left(2b^2 - 3\frac{k_BT_0}{m}\right)}{5\left(b^2 - 2\frac{k_BT_0}{m}\right)\left(3b^2 - 7\frac{k_BT_0}{m}\right)},$$

$$r_8 = \frac{b^2\left(5b^4 - 18b^2\frac{k_BT_0}{m} + 17\left(\frac{k_BT_0}{m}\right)^2\right)}{5\left(b^2 - 2\frac{k_BT_0}{m}\right)\left(3b^2 - 7\frac{k_BT_0}{m}\right)}. \tag{49}$$

We also have closure

$$n_\alpha = \frac{5}{2(b^2-2)D_1}\left[\left(4b^{10} - 24b^8\left(\frac{k_BT_0}{m}\right) + 88b^6\left(\frac{k_BT_0}{m}\right)^2 - 216b^4\left(\frac{k_BT_0}{m}\right)^3 + 196b^2\left(\frac{k_BT_0}{m}\right)^4\right)q_\alpha - \left(6b^8 - 89b^6\left(\frac{k_BT_0}{m}\right) + 448b^4\left(\frac{k_BT_0}{m}\right)^2 - 931b^2\left(\frac{k_BT_0}{m}\right)^3 + 686\left(\frac{k_BT_0}{m}\right)^4\right)\hat{N}_{\beta\gamma\theta}\delta_{\alpha\beta\gamma\theta} - \left(6b^{10} - 24b^8\left(\frac{k_BT_0}{m}\right) + 18b^6\left(\frac{k_BT_0}{m}\right)^2\right)J_\alpha\left(\frac{k_BT_0}{m}\right)\right] \tag{50}$$

C. Sixth order moment

Finally, the evolution equations for the sixth order moments may be written as

$$\partial_t\psi + \partial_\alpha(r_1J_\alpha + r_2q_\alpha + r_3\hat{N}_{\beta\gamma\theta}\delta_{\alpha\beta\gamma\theta}) = -\frac{1}{\tau}(\psi - \psi^{\mathrm{eq}}), \tag{51}$$

where

$$\psi^{\mathrm{eq}} = \frac{3\left(b^4 + 23b^2\frac{k_BT_0}{m} - 49\left(\frac{k_BT_0}{m}\right)^2\right)}{b^2 - 2\frac{k_BT_0}{m}}\rho\left(\frac{k_BT_0}{m}\right)^2,$$

$$r_1 = -\frac{3b^6\left(b^2 - \frac{k_BT_0}{m}\right)\left(17b^6 - 24b^4\left(\frac{k_BT_0}{m}\right) - 187b^2\left(\frac{k_BT_0}{m}\right)^2 + 294\left(\frac{k_BT_0}{m}\right)^3\right)}{2\left(b^2 - 2\frac{k_BT_0}{m}\right)^2\left(4b^6 - 33b^4\left(\frac{k_BT_0}{m}\right) + 116b^2\left(\frac{k_BT_0}{m}\right)^2 - 147\left(\frac{k_BT_0}{m}\right)^3\right)}\left(\frac{k_BT_0}{m}\right), \tag{52}$$

$$r_2 = \frac{b^4\left(17b^{10} - 135b^8\left(\frac{k_BT_0}{m}\right) + 797b^6\left(\frac{k_BT_0}{m}\right)^2 - 3189b^4\left(\frac{k_BT_0}{m}\right)^3 + 6026b^2\left(\frac{k_BT_0}{m}\right)^4 - 4116\left(\frac{k_BT_0}{m}\right)^5\right)}{\left(b^2 - 2\frac{k_BT_0}{m}\right)^2\left(4b^6 - 33b^4\left(\frac{k_BT_0}{m}\right) + 116b^2\left(\frac{k_BT_0}{m}\right)^2 - 147\left(\frac{k_BT_0}{m}\right)^3\right)},$$

$$r_3 = -\frac{5b^2\left(b^2 - 7\frac{k_BT_0}{m}\right)\left(2b^2 - 7\frac{k_BT_0}{m}\right)\left(3b^2 - 7\frac{k_BT_0}{m}\right)\left(5b^2 - 3\frac{k_BT_0}{m}\right)}{4\left(b^2 - 2\frac{k_BT_0}{m}\right)\left(4b^6 - 33b^4\left(\frac{k_BT_0}{m}\right) + 116b^2\left(\frac{k_BT_0}{m}\right)^2 - 147\left(\frac{k_BT_0}{m}\right)^3\right)}. \tag{53}$$

The moment system described above [Eqs. (36)–(38), (41), (42), (44)–(48), and (51)] is equivalent to the original kinetic equation. Indeed, a very similar set of equations will be obtained if the Grad's 26-moment system is extended with the sixth order moment ψ as an independent variable. What is very different from the usual Grad's moment system is the choice of the variable itself. It is not really obvious why the Grad's 26-moment system should be extended by just one higher-order moment. Typically, when Grad's system is extended, one includes next higher-order moment (or some meaningful contraction of it) into the list of variables. In the present context, the choice of the 27th variable as ψ (which is a sixth order rather than a fifth order moment) emerged automatically from the choice of the lattice itself. Such unusual extensions of the Grad's moment system is a typical feature of the LB type equations [18], although significance of such extension is not yet clear. All one can say at this juncture is that, such unusual extension of the Grad's system leads to boundary condition in a natural way via discrete equivalence of diffusive boundary conditions [9].

VIII. HYDRODYNAMIC LIMIT

It is expected that discrete kinetic equation, in the hydrodynamic limit, which is limit of Knudsen number going to zero, will lead to Navier-Stokes type equation. The usual procedure to obtain the transport coefficients and the hydrodynamic equation is to do the Chapman-Enskog expansion of the kinetic equation [48]. In this procedure, one writes the distribution function f and its time derivative in the powers of Knudsen number, Kn.

The hydrodynamic variables are not expended and in order to define time-derivatives consistency condition is used, which means that the derivatives of all other variables are evaluated using chain rule via time derivatives of the conserved quantities. Thus, we have

$$\sigma^{(0)}_{\alpha\beta} = \frac{J_\alpha J_\beta}{\rho}, \quad \hat{Q}^{(0)}_{\alpha\beta\gamma} = \frac{J_\alpha J_\beta J_\gamma}{\rho^2}. \tag{54}$$

Using Eq. (36), we define time derivatives as

$$\partial_t^{(0)}\rho = -\partial_\alpha J_\alpha,$$

$$\partial_t^{(0)} J_\alpha = -\partial_\beta\left(\frac{J_\alpha J_\beta}{\rho} + \rho\frac{k_B T_0}{m}\delta_{\alpha\beta}\right), \tag{55}$$

the chain rule gives

$$\begin{aligned}\partial_t^{(0)}\sigma^{(0)}_{\alpha\beta} &= (\partial_t^{(0)}\rho)\left(\frac{\partial\sigma^{\rm eq}_{\alpha\beta}}{\partial\rho}\right) + (\partial_t^{(0)}J_\gamma)\left(\frac{\partial\sigma^{\rm eq}_{\alpha\beta}}{\partial J_\gamma}\right)\\ &= -\frac{J_\alpha J_\beta}{\rho^2}\partial_\alpha J_\alpha - \left(\frac{J_\alpha}{\rho}\delta_{\beta\gamma} + \frac{J_\beta}{\rho}\delta_{\alpha\gamma}\right)\\ &\quad\times\partial_\beta\left(\frac{J_\alpha J_\beta}{\rho} + \rho\frac{k_B T_0}{m}\delta_{\alpha\beta}\right).\end{aligned} \tag{56}$$

Also, using Eq. (37), we have

$$\partial_t^{(0)}\sigma^{(0)}_{\alpha\beta} + \partial_\gamma\hat{Q}^{(0)}_{\alpha\beta\gamma} + \frac{k_B T_0}{m}(\partial_\alpha J_\beta + \partial_\beta J_\alpha) = -\sigma^{(1)}_{\alpha\beta}, \tag{57}$$

which can be simplified using Eq. (56) to obtain

$$\sigma^{(1)}_{\alpha\beta} = -\rho\frac{k_B T_0}{m}\left(\partial_\alpha\frac{J_\beta}{\rho} + \partial_\beta\frac{J_\alpha}{\rho}\right). \tag{58}$$

which means in the hydrodynamic limit, we do recover the Navier-Stokes equation for an isothermal model as

$$\partial_t\rho + \partial_\alpha J_\alpha = 0,$$

$$\partial_t J_\alpha + \partial_\beta\left(\frac{J_\alpha J_\beta}{\rho} + \rho\frac{k_B T_0}{m}\delta_{\alpha\beta}\right) = \partial_\beta\left[\mu\left(\partial_\alpha\frac{J_\beta}{\rho} + \partial_\beta\frac{J_\alpha}{\rho}\right)\right], \tag{59}$$

where the viscosity coefficient is $\mu = \tau\rho k_B T_0/m$. The important thing to notice here is that only $\sigma^{\rm eq}_{\alpha\beta}$ and $\hat{Q}^{\rm eq}_{\alpha\beta\gamma}$ appear in the first-order expansion. So, it is sufficient that the equilibrium values of those match with those obtained from the Maxwell-Boltzmann distribution. Thus, it confirms that the ansatz 1 is correct.

A similar computation with the energy conserving model recover the equation of motion as a Navier-Stokes-Fourier system.

$$\partial_t\rho + \partial_\alpha J_\alpha = 0,$$

$$\begin{aligned}\partial_t J_\alpha + \partial_\beta\left(\frac{J_\alpha J_\beta}{\rho} + \rho\frac{k_B T_0}{m}\delta_{\alpha\beta}\right)\\ = \partial_\beta\left(\mu\left(\partial_\alpha\frac{J_\beta}{\rho} + \partial_\beta\frac{J_\alpha}{\rho}\right) - \frac{2}{3}\partial_\gamma\frac{J_\gamma}{\rho}\delta_{\alpha\beta}\right),\end{aligned}$$

$$\begin{aligned}\partial_t T + \frac{J_\alpha}{\rho}\partial_\alpha T + \frac{2T}{3}\partial_\alpha\frac{J_\alpha}{\rho}\\ = -\frac{2}{3\rho}\left\{\partial_\beta\left(\mu\frac{5}{2}\partial_\beta T\right) + \partial_\beta\frac{J_\alpha}{\rho}\left[\mu\left(\partial_\alpha\frac{J_\beta}{\rho} + \partial_\beta\frac{J_\alpha}{\rho}\right)\right.\right.\\ \left.\left. - \frac{2}{3}\partial_\gamma\frac{J_\gamma}{\rho}\delta_{\alpha\beta}\right]\right\}.\end{aligned} \tag{60}$$

IX. UNIDIRECTIONAL FLOW: STATIONARY SOLUTION

In order to verify the usefulness of the modified D3Q27, presented in this work, we chose to illustrate the stationary solutions of the models for pressure driven and Couette flows. We wish to compare the solution obtained with the current model with that obtained from the Boltzmann BGK solution. We have chosen this set-up as the Couette flow was earlier analyzed in detail using the LB equation (see for example [18]). It is known from there that Knudsen layer is predicted only by D2Q16 model, which in three dimension means a model with 64 discrete velocities. Thus, it is a good set up to compare the effectiveness of the current model.

A. Setup description and outline of solution

We consider the fluid to be enclosed by two parallel plates normal to z direction and separated by a distance of L. The bottom plate at $z=-L/2$ moves unidirectionally with the velocity $\{U_1,0,0\}$ while the top place at $z=L/2$ moves with velocity $\{U_2,0,0\}$. It is assumed that tube is infinitely long in x direction and constant density gradient is imposed in the x direction. We aim to find the steady state solution to the kinetic equation in this particular setup.

Integration of the steady state moment system is done under following three assumptions:

(i) The flow is unidirectional, where all the fields except density depend only on the z coordinate.

(ii) Mass does not flow through the walls.

(iii) For low Mach number flows, the nonlinearities can be ignored and it is sufficient to consider the linearized moment system.

As the result, we find the inner solution for all the moments. This inner solution is a parametric family that depends on yet undetermined constants of integrations.

In order to find the constants of integrations, we need to include the boundary condition, which is available in population representation. Thus, we either should transform the inner solution obtained earlier (in terms of moments) to population, or to find the moment representation at the boundary (where the relevant populations are taken from the boundary, and the rest from the inner population). Note that this solution is still dependent on the same constants of integrations. Matching this solution with the inner solution will give us the value of integration constant, and thus solving the entire problem. Here, solving for J_x will be prioritized. The same strategy is already used and elaborated in details in [49].

B. Inner solution to the unidirectional stationary moment system

In this part, we start with the assumption that the flow is in a steady state and is unidirectional (all the fields depend only on the z coordinate due to the nature of the setup, which is infinite in x and y directions) with the exception of ρ, which only depends on x direction. The continuity equation in this limit simplifies to $\partial_z J_z=0$, and the boundary condition (no mass leak from the wall) implies $J_z=0$. Further, the momentum conservation equation in the x-direction simplifies as

$$\sigma_{xz}=-\frac{dp_0}{dx}z+k_1, \tag{61}$$

where $p_0=\rho(k_BT_0/m)$. Here, we assume that the pressure drop, dp_0/dx, is a constant. Equations (37) and (41) may be reformulated in the following form:

$$\partial_z(h_1J_x+h_2q_x+h_3\hat{N}_{xyy}+h_4\hat{N}_{xzz})=-\frac{1}{\tau}\sigma_{xz},$$

$$\partial_z(h_5J_x+h_6q_x+h_7\hat{N}_{xyy}+h_8\hat{N}_{xzz})=-\frac{1}{\tau}\hat{R}_{xz}, \tag{62}$$

where $h_1,h_2,\ldots,h_8$ are constants. Equation (62) may be solved by eliminating N_{xyy} and N_{xzz} using the fact that

$$-\frac{4b^6-16b^4\frac{k_BT_0}{m}+22b^2\left(\frac{k_BT_0}{m}\right)^2}{10b^4-55b^2\frac{k_BT_0}{m}+70\left(\frac{k_BT_0}{m}\right)^2}\partial_z^2\hat{R}_{xz}$$
$$=-\frac{1}{\tau}\left(\partial_z\hat{N}_{xyy}-\frac{b^4-12b^2\frac{k_BT_0}{m}+21\left(\frac{k_BT_0}{m}\right)^2}{5\left(b^2-2\frac{k_BT_0}{m}\right)}\frac{k_BT_0}{m}\partial_zJ_x\right)$$

$$\frac{6b^6-24b^4\frac{k_BT_0}{m}+18b^2\left(\frac{k_BT_0}{m}\right)^2}{10b^4-55b^2\frac{k_BT_0}{m}+70\left(\frac{k_BT_0}{m}\right)^2}\partial_z^2\hat{R}_{xz}$$
$$=-\frac{1}{\tau}\left(\partial_z\hat{N}_{xzz}-\frac{b^4-12b^2\frac{k_BT_0}{m}+21\left(\frac{k_BT_0}{m}\right)^2}{5\left(b^2-2\frac{k_BT_0}{m}\right)}\frac{k_BT_0}{m}\partial_zJ_x\right), \tag{63}$$

and eliminating q_x using Eq. (38),

$$\partial_z^2\hat{R}_{xz}=-\frac{1}{\tau}\partial_z\left(q_x-\frac{5}{2}J_x\frac{k_BT_0}{m}\right). \tag{64}$$

We note that here we already incorporate the fact that $\partial_z^2\sigma_{xz}=0$, thus we have

$$-\tau\frac{b^2-3\frac{k_BT_0}{m}}{2b^2-7\frac{k_BT_0}{m}}\partial_z^2\hat{R}_{xz}+\frac{k_BT_0}{m}\partial_zJ_x=-\frac{1}{\tau}\sigma_{xz},$$

$$-\tau b^2\left(\frac{2b^4-8b^2\frac{k_BT_0}{m}+5\left(\frac{k_BT_0}{m}\right)^2}{2b^4-11b^2\frac{k_BT_0}{m}+14\left(\frac{k_BT_0}{m}\right)^2}\right)\partial_z^2\hat{R}_{xz}+7\left(\frac{k_BT_0}{m}\right)^2\partial_zJ_x$$
$$=-\frac{1}{\tau}\hat{R}_{xz}, \tag{65}$$

which has a solution for $\hat{R}_{xz}$ as

$$\hat{R}_{xz}=7\sigma_{xz}\frac{k_BT_0}{m}+A_1\sinh\left(\frac{z}{\sqrt{3}\eta\tau}\right)+A_2\cosh\left(\frac{z}{\sqrt{3}\eta\tau}\right), \tag{66}$$

where, A_1 and A_2 are just integration constants determined by the boundary condition (refer next section) and

$$\sqrt{3}\eta = \sqrt{\frac{b^4 - 4b^2\frac{k_BT_0}{m} + 6\left(\frac{k_BT_0}{m}\right)^2}{b^2 - 2\frac{k_BT_0}{m}}}. \tag{67}$$

Substituting Eq. (66) into Eq. (65), we solve for J_x,

$$J_x = \frac{dp_0}{dx}\frac{z^2}{2\tau} - \frac{k_1 z}{\tau} + k_2 + \frac{1}{\sqrt{3}\eta}\frac{b^2 - 3\frac{k_BT_0}{m}}{2b^2 - 7\frac{k_BT_0}{m}}\left[A_2 \sinh\left(\frac{z}{\sqrt{3}\eta\tau}\right) + A_1 \cosh\left(\frac{z}{\sqrt{3}\eta\tau}\right)\right]. \tag{68}$$

Here, we obtained a family of moments that is dependent on four integration constants (k_1, k_2, A_1, and A_2). To determine these, we need to specify boundary conditions at the walls. Note that this is an advantage of LB hierarchy, since it is well known that it is not possible to provide self-consistent boundary conditions for the other moments methods (such as the Grad's systems) [27]. In the present case, this is possible because the boundary conditions for the LB kinetic equations are formulated in terms of populations rather than moments [9].

C. Diffusive wall boundary condition

Boundary conditions for discrete velocity models are formulated in terms of distribution function. Thus, in order to apply boundary conditions, it is more convenient to come back from the moment representation to the distribution representation. For the present system, we apply the classical Maxwell's diffusive wall boundary condition. In this condition, particles that reach the wall are redistributed in a way consistent with the mass-balance and normal-flux condition,

$$f_i|_{\mathbf{c}\cdot\mathbf{n}>0} = \frac{\sum_{\mathbf{c}_j\cdot\mathbf{n}<0} |(\mathbf{c}_j\cdot\mathbf{n})| f_j}{\sum_{\mathbf{c}_j\cdot\mathbf{n}<0} |(\mathbf{c}_j\cdot\mathbf{n})| f_j^{eq}(\rho, \mathbf{U}_{\text{wall}})} f_i^{eq}(\rho, \mathbf{U}_{\text{wall}}), \tag{69}$$

where $\mathbf{n}$ is the inner normal at the wall, and $\mathbf{U}_{wall}$ is the wall velocity. This boundary condition redistributes the populations that reach the wall according to the equilibrium distribution of the population that leaves the wall.

Since the solution for the moments must be continuous, we should have the inner solution same as the result obtained from the boundary condition, where f_i is taken from Eq. (69) whenever $\mathbf{c}\cdot\mathbf{n}>0$ and taken from the Grad representation f_i (see Ref. [49]), if otherwise. With such definition of f_i, we can have boundary conditions by taking the moment of f_i with respect to c_{ix} and $c_{ix}c_{iz}^2$, on the top and bottom wall, respectively.

Since we have 4 equations and 4 unknowns, the system can be solved unambiguously. Substituting the inner solution and solving for the unknowns give rise to the following solutions:

$$k_1 = \frac{\rho\tau\Delta U\left\{b\left[\left(b^2 - 2\frac{k_BT_0}{m}\right)^{3/2} + 2\left(\frac{k_BT_0}{m}\right)^{3/2}\right]\cosh\left(\frac{z}{\sqrt{3}\eta\tau}\right) + b^2\sqrt{b^4 - 4b^2\frac{k_BT_0}{m} + 6\left(\frac{k_BT_0}{m}\right)^2}\sinh\left(\frac{z}{\sqrt{3}\eta\tau}\right)\right\}}{\mathcal{D}}$$

$$A_1 = \frac{\rho\tau\Delta U 2b\left(2b^2 - 7\frac{k_BT_0}{m}\right)\left(\sqrt{b^2 - 2\frac{k_BT_0}{m}} - \sqrt{\frac{k_BT_0}{m}}\right)}{\mathcal{D}} \tag{70}$$

$$k_2 = -\frac{dp_0}{dx}\left[\frac{L^2}{8\tau k_BT_0}\frac{m}{} + \frac{1}{2b}\left(2 + \sqrt{b^2\frac{m}{k_BT_0} - 2}\right)L + 2\tau\right] + \frac{U_1+U_2}{2}\frac{1}{\mathcal{D}_P}\frac{dp_0}{dx}\left\{\left[\left(\frac{k_BT_0}{m} - b^2\right)\sqrt{b^2 - 2\frac{k_BT_0}{m}} + 2\left(b^2 - 2\frac{k_BT_0}{m}\right)\sqrt{\frac{k_BT_0}{m}}\right]L + 2b\left(b^2 - 3\frac{k_BT_0}{m}\right)\times\left(\sqrt{\frac{k_BT_0}{m}} - \sqrt{b^2 - 2\frac{k_BT_0}{m}}\right)\tau\right\}\sinh\left(\frac{L}{2\sqrt{3}\eta\tau}\right) \tag{71}$$

$$A_2 = \frac{2b^2 - 7\frac{k_BT_0}{m}}{\mathcal{D}_P}\frac{dp_0}{dx}\left[b\left(\sqrt{b^2\frac{m}{k_BT_0} - 2} - 1\right)L + 2b^2\left(\frac{b^2\frac{m}{k_BT_0} - 3}{\sqrt{b^2\frac{m}{k_BT_0} - 2}}\right)\tau\right] \tag{72}$$

where, the denominators, $\mathcal{D}$ and $\mathcal{D}_P$ are, respectively, defined as

TABLE I. Constants appearing in a generic expression for dimensional shear stress [Eq. (77)].

	Υ^1	Υ^2	Υ^3	Υ^4	Υ^5	Υ^6	Υ^7
Basis 1	6.93489	0.303784	7.23518	4.79193	7.1253	4.99943	8.82956
Basis 2	18.1766	0.217371	6.95667	12.5598	21.9968	4.80697	8.96816

$$\mathcal{D} = \left\{ b\left[\left(b^2 - 2\frac{k_B T_0}{m} \right)^{3/2} + 2\left(\frac{k_B T_0}{m} \right)^{3/2} \right] \sqrt{\frac{m}{k_B T_0}} L + 2b^4 \tau \right\} \cosh\left(\frac{z}{\sqrt{3}\eta\tau} \right) + \sqrt{b^4 - 4b^2 \frac{k_B T_0}{m} + 6\left(\frac{k_B T_0}{m} \right)^2} \left[b^2 \sqrt{\frac{m}{k_B T_0}} L + 2b\left(2\sqrt{\frac{k_B T_0}{m}} + \sqrt{b^2 - 2\frac{k_B T_0}{m}} \right) \tau \right] \sinh\left(\frac{z}{\sqrt{3}\eta\tau} \right) \tag{73}$$

$$\mathcal{D}_P = b^2 \sqrt{b^4 - 4b^2 \frac{k_B T_0}{m} + 6\left(\frac{k_B T_0}{m} \right)^2} \cosh\left(\frac{L}{2\sqrt{3}\eta\tau} \right) + b\left[\left(b^2 - 2\frac{k_B T_0}{m} \right)^{3/2} + 2\left(\frac{k_B T_0}{m} \right)^{3/2} \right] \sinh\left(\frac{L}{2\sqrt{3}\eta\tau} \right). \tag{74}$$

We note that up to here, both on-lattice scheme and off-lattice scheme are valid. It is easy to check that for $b=\sqrt{3}$, we recover back the characteristic result of $D3Q27$. In the next section, we will substitute the parameter of off-lattice scheme directly to get some numerics to compare with the available data. We also define Knudsen number as:

$$\mathrm{Kn} = \frac{\tau}{L}\sqrt{\frac{3k_B T_0}{m}}. \tag{75}$$

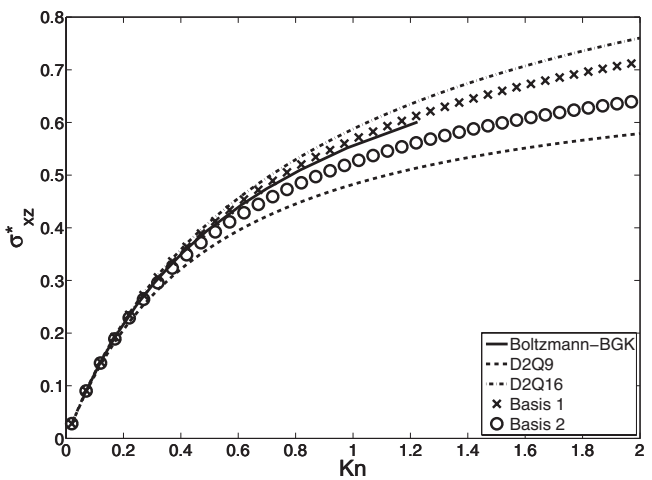

FIG. 2. Shear stress profile for Couette flow.

X. COUETTE FLOW

The shear stress is the quantity of interest in the Couette flow. We define dimensionless shear stress consistent with Ref. [50] as

$$\sigma^*_{xz} = -\frac{\sigma_{xz}}{\rho(U_2 - U_1)}\sqrt{\frac{2\pi m}{k_B T_0}}. \tag{76}$$

This dimensionless shear stress for the first and second basis is given as per the following equation:

$$\sigma^*_{xz} = \frac{\left(\Upsilon^1 \coth\left(\frac{\Upsilon^2}{\mathrm{Kn}} \right) + \Upsilon^3 \right)\mathrm{Kn}}{(\Upsilon^4 + \Upsilon^5 \mathrm{Kn})\coth\left(\frac{\Upsilon^2}{\mathrm{Kn}} \right) + (\Upsilon^6 + \Upsilon^7 \mathrm{Kn})}. \tag{77}$$

In Table I, we have listed the constants $\Upsilon^1, \ldots, \Upsilon^7$ appearing in the dimensionless shear stress equation. This dimensionless shear stress is plotted in Fig. 2.

The convergence of the discrete Boltzmann equation toward its continuous counterpart can also be analyzed via solution at $\mathrm{Kn} \to \infty$. For example, we know that the infinite Knudsen limit of the dimensionless shear stress $\nu^{\infty}_{\mathrm{eff}}$ for the Boltzmann-BGK equation is equal to unity. The comparison is tabulated in Table II. From the table, it is evident that the current model with the first basis is converging much faster to the Boltzmann equation compared to any other approximations. Furthermore, the quality of result also suggests that the model with the first basis performs much better compared to the second one. Yet another useful quantity which shows nontrivial behavior in high Knudsen number cases is nondimensional centerline velocity gradient Y, defined as

$$Y = 1 - \frac{1}{U_2 - U_1}\left(\frac{du_x}{dz/L} \right)_{z=0} = 1 + \frac{m}{k_B T_0}\left(\frac{A_1}{\eta \mathrm{Kn}} - \frac{k_1}{\mathrm{Kn}}\sqrt{\frac{3k_B T_0}{m}} \right). \tag{78}$$

TABLE II. Comparison of effective shear viscosity at $\mathrm{Kn} \to \infty$ between the Boltzmann-BGK model and various LB models.

Model	$\nu^{\infty}_{\mathrm{eff}}$
Boltzmann-BGK	1
$D2Q9$	0.723
$D2Q16$	1.113
Current Basis 1	0.973
Current Basis 2	0.826

TABLE III. Deviation of nondimensional velocity gradient from Navier-Stokes value for the current models, $D2Q9$ [49], and the Boltzmann-BGK kinetic equations [50]. Percentage error of the value of deviation is relative to Boltzmann-BGK value.

	Values				Error (%)		
Kn	Boltzmann-BGK	$D2Q9$	Basis 1	Basis 2	$D2Q9$	Basis 1	Basis 2
0.06124	0.09134	0.10911	0.09152	0.09973	19.450	0.1971	9.185
0.12247	0.1648	0.1968	0.1749	0.1860	19.387	5.775	12.864
0.17496	0.2136	0.2592	0.2384	0.2480	21.358	10.403	16.104
0.24495	0.2664	0.3288	0.3096	0.3165	23.427	13.953	18.806
0.30619	0.3041	0.3798	0.3611	0.3663	24.890	15.785	20.454
0.61237	0.4290	0.5509	0.5301	0.5332	28.408	19.071	24.289
0.81650	0.4821	0.6202	0.5986	0.6024	28.646	19.462	24.953
1.22474	0.5556	0.7101	0.6880	0.6930	27.808	19.244	24.730

The result and its relative error are tabulated in Table III. From the table, it is evident that the current model with the first basis is converging much faster to the Boltzmann equation compared to any other approximations. Furthermore, the quality of result also suggest that the model with first basis performs much better compared to the second one.

XI. KNUDSEN PARADOX

It is well known that for the pressure driven flow, so called "Knudsen paradox" behavior where the flow rate shows a minimum as a function of the Knudsen number. In the present section, we compare the result from the present discrete velocity model with the continuous Boltzmann-BGK equation as well as existing Hermite based lattice Boltzmann models. For pressure driven flows, we can set $U_1=U_2=0$ in the general solution Eq. (68). In this setup the quantity of interest is the dimensionless flow rate Q defined as

$$Q = -\frac{1}{L^2}\left(\frac{dp_0}{dx}\right)^{-1}\sqrt{\frac{2k_BT_0}{m}}\int_{z=-L/2}^{z=L/2} J_x dz. \tag{79}$$

In order to compare present result with the existing result in the literature, we follow the convention in the literature and redefined Knudsen number into $\widehat{\mathrm{Kn}}$, such that $\widehat{\mathrm{Kn}}=\mathrm{Kn}\sqrt{2/3}$. From the Boltzmann-BGK equation, we know that in this particular setup, the dimensionless flow rate defined in Eq. (79) theoretically should have a minimum at $\widehat{\mathrm{Kn}}\approx 1$ [51].

Here, we write the expression for dimensionless flow rate in a generic way and construct Table IV as a comparison with different findings.

$$Q = \frac{1}{6\widehat{\mathrm{Kn}}} + \Upsilon_1 + \Upsilon_2\widehat{\mathrm{Kn}} - \frac{\Upsilon_3 + \Upsilon_4\widehat{\mathrm{Kn}} + \Upsilon_5\widehat{\mathrm{Kn}}^2}{\Upsilon_6 \coth\left(\frac{\Upsilon_7}{\widehat{\mathrm{Kn}}}\right) + 1} \tag{80}$$

It can be shown that the profile given by first Basis indeed exhibits Knudsen paradox with Knudsen minimum occurring at $\mathrm{Kn}\approx 0.5886$. For the second basis, with the flat profile, which has no minimum and distinct value in the limit of Knudsen number going to infinity. Thus, similar to $D2Q16$ model, the second basis in the present case do not exhibit Knudsen paradox behavior. We can see that the first term of the flow rate (order of $\widehat{\mathrm{Kn}}^{-1}$) basically represents the Navier-Stokes limit. In Table IV and using present notation, we have compared the result with the Cercignani quadratic approximation using the slip flow model. This has previously used in comparing $D2Q9$ model in [49].

Finally, we would like to comment on the other possible models for microflow. Recently, the Grad's moment method was modified to obtain the $R13$ equation [53,54], for which boundary condition was developed in Ref. [52]. In recent year, it has been shown that $R13$ with proper boundary condition gives as good result as the LB method for microflows [52]. The constants appearing in the expression of the flow rate using the $R13$ approach as in [52] have been tabulated in Table IV.

From Fig. 3, it is visible that our current approach with the first basis gives an almost exact agreement with the result

TABLE IV. Constants appearing in a generic expression for dimensionless flow rate [Eq. (80)].

Ref.	Υ_1	Υ_2	Υ_3	Υ_4	Υ_5	Υ_6	Υ_7
Basis 1	1.08152	2.0	0.17096	2.06084	6.21071	1.04330	0.248039
Basis 2	1.14248	2.0	0.06999	2.00291	11.40948	1.01249	0.177483
Ref. [49]	1.01617	1.5324					
Ref. [52]	0.97108	1.1333	0.0848528	0.6	1.06065	0.931695	0.527046

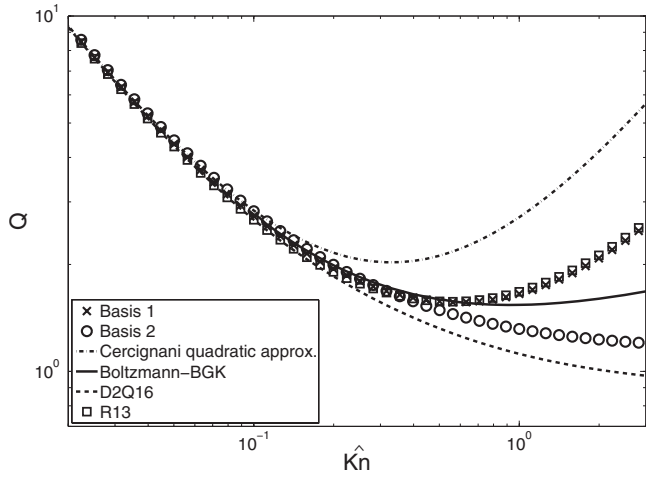

FIG. 3. Flow rate Q as a function of the resized Knudsen number $\widehat{\mathrm{Kn}}$ for Poiseuille flow.

of R13. Further, it behaves much better than $D2Q16$ model used in literature as the present model can capture boundary layer as well as Knudsen minimum.

XII. NUMERICAL ILLUSTRATION

In this section, numerical result corresponding to the Couette flow simulations has been illustrated for on-lattice and off-lattice representations with $D3Q27$ velocity model. The numerical setup has been explained earlier in Sec. IX. In the computational domain the moving walls are considered to be located at $z=0$ and $z=L$. Here, two representative Knudsen numbers (Kn=0.5 and 1.0) are considered and an isothermal equilibrium distribution function given by Eq. (8) is used. The flow Mach number is kept constant (Ma=0.075) in these simulation runs. A diffusive wall boundary condition given by Eq. (69) is used for walls in z direction and a periodic boundary condition is employed in x direction. The computational procedure is described as follows:

(i) A formal short-time solution for Eq. (2) may be written by evaluating the usual BGK collision kernel $[\Omega_i=1/\tau(f_i^{\mathrm{eq}}-f_i)]$, using the trapezoidal rule (assuming linear interpolation)

$$f_i(\mathbf{x}+\mathbf{c}\Delta t,\mathbf{c},t+\Delta t)=f_i(\mathbf{x},\mathbf{c},t)+\frac{\Delta t}{2}\{\Omega_i[f_i(\mathbf{x},\mathbf{c},t)]+\Omega_i[f_i(\mathbf{x}+\mathbf{c}\Delta t,\mathbf{c},t+\Delta t)]\}+\mathcal{O}(\Delta t^3). \tag{81}$$

(ii) First, in order to create an efficient explicit numerical scheme we transform the distribution functions, f_i, in terms of g_i using the following:

$$g_i(\mathbf{x},\mathbf{c},t)=f_i(\mathbf{x},\mathbf{c},t)-\frac{\Delta t}{2\tau}[f_i^{\mathrm{eq}}(\mathbf{x},\mathbf{c},t)-f_i(\mathbf{x},\mathbf{c},t)] \tag{82}$$

and hence the corresponding LB evolution equation using the above transformation is

$$g_i(\mathbf{x}+\mathbf{c}\Delta t,t+\Delta t)=g_i(\mathbf{x},t)+2\beta\{g_i^{\mathrm{eq}}[g(\mathbf{x},t)]-g_i(\mathbf{x},t)\}, \tag{83}$$

where, $\beta=\Delta t/(2\tau+\Delta t)$.

(iii) The Eq. (83) may be written as consisting of two-steps, namely, local-collision and streaming. The postcollision distribution functions ($g_i^\star$) may be found as

$$g_i^\star(\mathbf{x},t)=g_i(\mathbf{x},t)+2\beta[g_i^{\mathrm{eq}}(\mathbf{x},t)-g_i(\mathbf{x},t)], \tag{84}$$

and thus computed $g_i^\star$'s may then be streamed for the usual on-lattice representation as

$$g_i(\mathbf{x},t+\Delta t)=g_i^\star(\mathbf{x}-\mathbf{c}\Delta t,t). \tag{85}$$

(iv) Further, the grid-spacing, $\delta x=\delta y=\delta z$ and the time-step, $\Delta t=\delta x/b$ is chosen.

(v) In an off-lattice simulation, the usual streaming procedure [Eq. (85)] is performed for the distribution functions corresponding to the energy shell, b. Hence, a convection term contribution needs to be computed for the energy shells apart from b. This contribution is evaluated after calculating the postcollision distribution functions using Eq. (84) as

$$g_i(\mathbf{x},t+\Delta t)\approx g_i^\star(\mathbf{x},t)-\frac{\partial g_i^\star}{\partial x_\alpha}c_{i\alpha}\Delta t\approx g_i^\star(\mathbf{x},t)+\frac{\mp g_i^\star(\mathbf{x}\mp c_{i\alpha}\Delta t,t)\pm g_i^\star(\mathbf{x},t)}{\delta x}|c_{i\alpha}|\Delta t. \tag{86}$$

Here, a quasi-two-dimensional approximation has been made. This is because, the illustrative example under consideration is an unidirectional. The approximation implies $\partial g_i/\partial y=0$ and hence no convection in y direction. The gradients of the distribution functions are evaluated using a first-order upwind scheme. The scheme is stable and sufficiently accurate. Further, we found that the use of central-difference scheme is unstable. Here, we do acknowledge the fact that for a full three-dimensional simulations, estimation of the gradients of g_i's is an involved task.

A computational mesh comprises a total of $(16\times1\times128)$ number of lattice points. In Fig. 4, the x-directional velocity (u) normalized with respect to the positive x-directional wall velocity (U_{wall}) has been plotted versus the z coordinate. From Fig. 4, a very good comparison of the numerical results (shown using lines) with the analytical solution (shown using symbols) obtained from Sec. X) may be clearly seen. Further, a slope of the curve predicted using the off-lattice representation is observed to be larger than that of on-lattice model. From this numerical exercise, we conclude that an off-lattice LB ($D3Q27$) is easily implementable with a good accuracy for finite Knudsen flows.

XIII. OUTLOOK

In the present work, an alternate framework to create discrete velocity set is suggested. It is shown that in this framework the entropic formulation of the LB method can be naturally extended to obtain a discrete velocity set with a given accuracy. As an example, a 27-velocity LB model with the

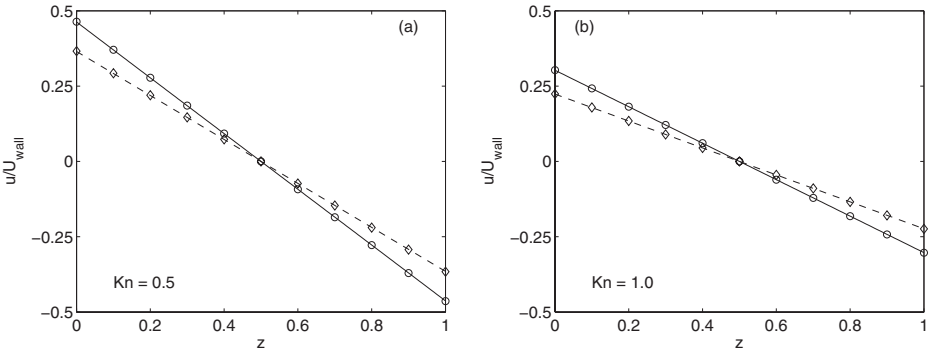

FIG. 4. Comparison of the analytical solution (symbols; ◇: on-lattice, ○: off-lattice representation) with the numerical data (dotted line: on-lattice, solid line: off-lattice). (a) Kn=0.5; (b) Kn =1.0.

Galilean-invariant hydrodynamic limit is derived. As compared to existing model, the advantage of the current model is that it not only captures the Knudsen layer effect which does not exist in $D2Q9$ model, it also has a Knudsen minimum which does not exist in $D2Q16$ model. Therefore, it combines the advantages of $D2Q9$ and $D2Q16$ at the same time. Thus to conclude, we have presented a novel model which can predict both Knudsen layer effect and Knudsen paradox, with rather minimal number of discrete velocities for three-dimensional system. The presented scheme has high efficiency for realistic applications due to the minimal number of discrete velocities. It gives an edge for quantitative computation in engineering application, given some modification for computational purpose (due to the fact that it is off-lattice). In part II of this work, we shall demonstrate the usefulness of the current model in the case of two component mixture.

ACKNOWLEDGMENTS

We would like to thank Dr. Xiaowen Shan for insightful comments. SA and D.V. Patil are thankful to Department of Science and Technology (DST), India for providing computational resources.

[1] H. Chen, S. Chen, and W. H. Matthaeus, Phys. Rev. A **45**, R5339 (1992).
[2] Y. H. Qian, D. d'Humieres, and P. Lallemand, EPL **17**, 479 (1992).
[3] F. Higuera, S. Succi, and R. Benzi, EPL **9**, 345 (1989).
[4] R. Benzi, S. Succi, and M. Vergassola, Phys. Rep. **222**, 145 (1992).
[5] S. Succi, *The Lattice Boltzmann Equation for Fluid Dynamics and Beyond* (Oxford University Press, Oxford, 2001).
[6] H. Chen, S. Kandasamy, S. Orszag, R. Shock, S. Succi, and V. Yakhot, Science **301**, 633 (2003).
[7] S. Chen and G. D. Doolen, Annu. Rev. Fluid Mech. **30**, 329 (1998).
[8] S. Succi, I. V. Karlin, and H. Chen, Rev. Mod. Phys. **74**, 1203 (2002).
[9] S. Ansumali and I. V. Karlin, Phys. Rev. E **66**, 026311 (2002).
[10] X. Shan and X. He, Phys. Rev. Lett. **80**, 65 (1998).
[11] S. Ansumali, I. V. Karlin, and H. C. Öttinger, EPL **63**, 798 (2003).
[12] S. Succi, Phys. Rev. Lett. **89**, 064502 (2002).
[13] B. Li and D. Y. Kwok, Phys. Rev. Lett. **90**, 124502 (2003).
[14] X. D. Niu, C. Shu, and Y. Chew, EPL **67**, 600 (2004).
[15] S. Ansumali and I. V. Karlin, Phys. Rev. Lett. **95**, 260605 (2005).
[16] V. Sofonea and R. Sekerka, J. Comput. Phys. **207**, 639 (2005).
[17] J. Horbach and S. Succi, Phys. Rev. Lett. **96**, 224503 (2006).
[18] S. Ansumali, I. V. Karlin, S. Arcidiacono, A. Abbas, and N. I. Prasianakis, Phys. Rev. Lett. **98**, 124502 (2007).
[19] S. H. Kim, H. Pitsch, and I. D. Boyd, Phys. Rev. E **79**, 016702 (2009).
[20] S. Ansumali, Ph.D. thesis, ETH Zurich, 2004).
[21] S. S. Chikatamarla, Ph.D. thesis, ETH Zurich, 2008.
[22] S. S. Chikatamarla and I. V. Karlin, Phys. Rev. Lett. **97**, 190601 (2006).
[23] S. S. Chikatamarla and I. V. Karlin, Phys. Rev. E **79**, 046701 (2009).
[24] X. Nie, X. Shan, and H. Chen, EPL **81**, 34005 (2008).
[25] S. S. Chikatamarla, C. E. Frouzakis, I. V. Karlin, A. G. Tomboulides, and K. B. Boulouchos, J. Fluid Mech. **656**, 298 (2010).
[26] T. Abe, J. Comput. Phys. **131**, 241 (1997).
[27] H. Grad, Commun. Pure Appl. Math. **2**, 331 (1949).
[28] I. V. Karlin, A. N. Gorban, S. Succi, and V. Boffi, Phys. Rev. Lett. **81**, 6 (1998).
[29] A. J. Wagner, EPL **44**, 144 (1998).
[30] I. V. Karlin, A. Ferrante, and H. C. Öttinger, EPL **47**, 182 (1999).
[31] B. M. Boghosian, J. Yepez, P. V. Coveney, and A. Wagner, Proc. R. Soc. London, Ser. A **457**, 717 (2001).
[32] B. M. Boghosian, P. J. Love, P. V. Coveney, I. V. Karlin, S. Succi, and J. Yepez, Phys. Rev. E **68**, 025103 (2003).
[33] A. Kogan, Prikl. Math. Mech **29**, 122 (1965).
[34] P. C. Philippi, L. A. Hegele, L. O. E. dos Santos, and R. Surmas, Phys. Rev. E **73**, 056702 (2006).
[35] X. Shan, X. Yuan, and H. Chen, J. Fluid Mech. **550**, 413 (2006).
[36] S. Arcidiacono, J. Mantzaras, S. Ansumali, I. V. Karlin, C. Frouzakis, and K. B. Boulouchos, Phys. Rev. E **74**, 056707 (2006).
[37] S. H. Kim, H. Pitsch, and I. D. Boyd, J. Comput. Phys. **227**,

8655 (2008).
[38] A. H. Stroud, *Approximate Calculation of Multiple Integrals* (Prentice-Hall, Englewood Cliffs, NJ, 1971).
[39] X. Shan, Phys. Rev. E **81**, 036702 (2010).
[40] J. E. Broadwell, J. Fluid Mech. **19**, 401 (1964).
[41] U. Frisch, B. Hasslacher, and Y. Pomeau, Phys. Rev. Lett. **56**, 1505 (1986).
[42] P. L. Bhatnagar, E. P. Gross, and M. Krook, Phys. Rev. **94**, 511 (1954).
[43] X. He and L. S. Luo, Phys. Rev. E **55**, R6333 (1997).
[44] X. He and L. S. Luo, Phys. Rev. E **56**, 6811 (1997).
[45] Y. H. Qian and S. A. Orszag, EPL **21**, 255 (1993).
[46] B. Keating, G. Vahala, J. Yepez, M. Soe, and L. Vahala, Phys. Rev. E **75**, 036712 (2007).
[47] N. Ashcroft and N. Mermin, *Solid State Physics* (Harcourt College Publisher, New York, 1976).
[48] S. Chapman and T. G. Cowling, *The Mathematical Theory of Non-Uniform Gases* (Cambridge University Press, Cambridge, England, 1970).
[49] W. P. Yudistiawan, S. Ansumali, and I. V. Karlin, Phys. Rev. E **78**, 016705 (2008).
[50] D. R. Willis, Phys. Fluids **5**, 127 (1962).
[51] C. Cercignani, *Theory and Application of the Boltzmann Equation* (Scottish Academic Press, Edinburgh, 1975).
[52] H. Struchtrup and M. Torrilhon, Phys. Rev. Lett. **99**, 014502 (2007).
[53] I. V. Karlin, A. N. Gorban, G. Dukek, and T. F. Nonnenmacher, Phys. Rev. E **57**, 1668 (1998).
[54] H. Struchtrup and M. Torrilhon, Phys. Fluids **15**, 2668 (2003).